

Supporting Information

Significantly Promotion the Lithium-Ion Transport Performances of MOFs Based Electrolytes via a Strategy of Introducing Fluoro-group in Crystal Frameworks

Jia Guo, Xin Wang, Lu Shi and Zhiliang Liu*

College of Chemistry and Chemical Engineering, Inner Mongolia University, Hohhot 010021, P.R. China.

E-mail: cezliu@imu.edu.cn

Contents

Experimental section

Electrochemical Studies

Fig. S1 EDX of the as-synthesized Cu-MOF.

Fig. S2 EDX of the as-synthesized Cu-MOF-F₄.

Fig. S3 ¹H NMR spectra of digested (a) Cu-MOF-F₁, (b) Cu-MOF-F₂, (c) Cu-MOF-F₃, and (d) Cu-MOF-F₅ in [D₆] DMSO.

Fig. S4 The TGA of the as-synthesized Cu-MOF and Cu-MOF-F₄.

Fig. S5 EIS of (a) Cu-MOF, (b) Cu-MOF-F₁, (c) Cu-MOF-F₂, (d) Cu-MOF-F₃, (e) Cu-MOF-F₄, and (f) Cu-MOF-F₅ electrolyte at temperatures from -40 to 110 °C.

Fig. S6 Chronoamperometric curves and EIS curves of (a) Cu-MOF, (b) Cu-MOF-F₁, (c) Cu-MOF-F₂, (d) Cu-MOF-F₃, and (e) Cu-MOF-F₅ electrolyte before and after polarization.

Fig. S7 LSV profiles of Cu-MOF-F_x SSEs sandwiched between Li foil and SS electrodes at -40°C.

Table S1 Tabulated synthetic conditions.

Table S2 Electrolyte uptake of various samples.

Table S3 Electrochemical performance of as-prepared Cu-MOF and Cu-MOF-F_x at different temperature.

Table S4 Summary of conductivity of lithium ions electrolytes at low temperatures.

References

Experimental Section

Synthesis of Cu-MOF: Cu-MOF crystals were synthesized according to the reported in the literature.¹ $\text{Cu}(\text{NO}_3)_2 \cdot 3\text{H}_2\text{O}$ (0.41 mmol, 99 mg) and isonicotinic acid (INA) (0.082 mmol, 10 mg) were dissolved in a mixture of 2 mL of N-methyl-2-pyrrolidone (NMP), 0.7 mL of deionized water and 0.3 mL of nitric acid ($1 \text{ mol} \cdot \text{L}^{-1}$) in a 10 mL vial. After it was sonicated for 10 min, the subsequent solution was heated at $100 \text{ }^\circ\text{C}$ for 84 h. The resulting blue single crystals were left to cool at room temperature, then washed three times with NMP and dried in a vacuum oven for 6 h at $60 \text{ }^\circ\text{C}$.

Synthesis of Cu-MOF- F_x ($x=1,2,3,4,5$): Cu-MOF- F_1 , Cu-MOF- F_2 , Cu-MOF- F_3 , Cu-MOF- F_4 , and Cu-MOF- F_5 was obtained by the same procedure but replacing the INA with different amount of FINA listed in Table. S1.

Preparation of solid electrolyte membranes: MOF nanoparticles were dispersed in an isopropanol and PTFE aqueous solution (MOF : PTFE = 9 : 1) by hand milling and the mixture was rolled into a thin film. Then, the membranes were cut into desirable sized free-standing and flexible pieces with a thickness of about $250 \text{ }\mu\text{m}$ (diameter of 16 mm). The obtained flexible membranes were dried in a vacuum at $80 \text{ }^\circ\text{C}$ overnight, and then stored in an argon filled glove box ($\text{H}_2\text{O} \leq 0.01 \text{ ppm}$, $\text{O}_2 \leq 0.01 \text{ ppm}$). The solid electrolyte was soaked in 1 M LiPF_6 solution for 24 h to adsorb a certain amount of Li^+ , pressed to extrude any excess liquid electrolyte, wiped with filter paper and argon-dried for 5 min.

Inductively coupled plasma emission spectroscopy (ICP) measurements demonstrated that the content of LiPF_6 in electrolyte membrane (Cu-MOF- F_4) was 16.29 %. The residual solvent was quantified by weighing the mass of the electrolyte membrane before and after immersion in the LiPF_6 solution. Taking Cu-MOF- F_4 as examples of parallel testing of two groups, the detailed data was shown in the Table S2, where M_1 and M_2 are the mass of the sample before and after adsorbing the LiPF_6 solution, respectively. $M_2 - M_1$ is the mass of ($\text{LiPF}_6 + \text{solvent}$) in electrolyte membrane. The percentage of residual solvent content in electrolyte membrane can be determined to be about $\sim 4.6 \%$.

Materials characterization

Powder X-ray diffraction (PXRD) measurement was recorded on an Empyrean PANalytical diffractometer with Cu K α radiation ($\lambda = 1.5406 \text{ \AA}$) at 40 mA and 40 kV. Scanning electron microscopy (SEM) images were obtained using a Hitachi S-4800 Scanning electron microscopy. Thermogravimetric analysis (TGA) was performed on a NETZSCH TG 209F3 with a heating rate of $10 \text{ }^\circ\text{C min}^{-1}$ under a nitrogen atmosphere.

The calculation method of FINA ratio

Taking Cu-MOF-F_x as an example, 10 mg of the sample was digested with 1 M NaOH, followed by the addition of 0.5 ml of DMSO-d₆ directly to the mixture, and the ¹H NMR spectra were tested. The amount of two ligands can be calculated by comparing the integral area of the peak of FINA(A1) with that of the INA(A2) characteristic peak.

The product yield can be calculated by the equation:

$$\text{Ratio}_{(A1)} = \frac{A1}{A1 + A2/2} \times 100\%$$

Electrochemical Studies

Ionic conductivity of the electrolyte membranes was measured by electrochemical impedance spectroscopy (EIS) with frequency ranging from 1 Hz to 1 MHz. The solid electrolyte membranes were sandwiched between two stainless steel electrodes. The ionic conductivity was calculated according to the following formula (1):

$$\sigma = \frac{L}{R \times S} \#(1)$$

where L (cm), R (ohm) and S (cm²) are the thickness, bulk resistance and the area of the membrane, respectively.

The activation energy (E_a) was obtained from the slope of the Arrhenius plot using formula (2):

$$\sigma = A e^{(-E_a/RT)} \#(2)$$

where A and T represent the pre-exponential factor and the Kelvin temperature, respectively.

The Li^+ transference number (t_{Li^+}) was measured by combining an A.C. impedance measurement and an amperometric *i-t* curve measurement using Li|electrolyte|Li cells.

The t_{Li^+} can be calculated according to the following formula (3):

$$t_{\text{Li}^+} = \frac{I_{SS} (\Delta V - I_0 R_0)}{I_0 (\Delta V - I_{SS} R_{SS})} \quad \#(3)$$

Where ΔV is the DC polarization voltage, and I_0 and I_{SS} are the initial stable currents before and after polarization, respectively. R_0 and R_{SS} are the initial stable resistance before and after polarization.

The electrochemical window was determined by cyclic voltammetry (CV) and linear sweep voltammetry (LSV) using SS|electrolyte|Li cells with the voltage range of 0 to 7 V and the scanning rate of 1 mV s^{-1} .

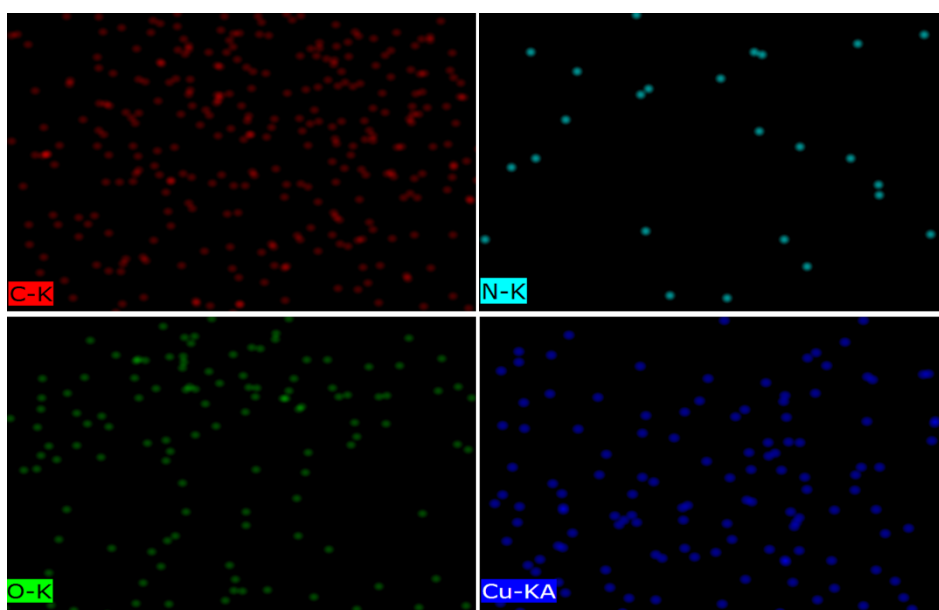


Fig. S1 EDX of the as-synthesized Cu-MOF.

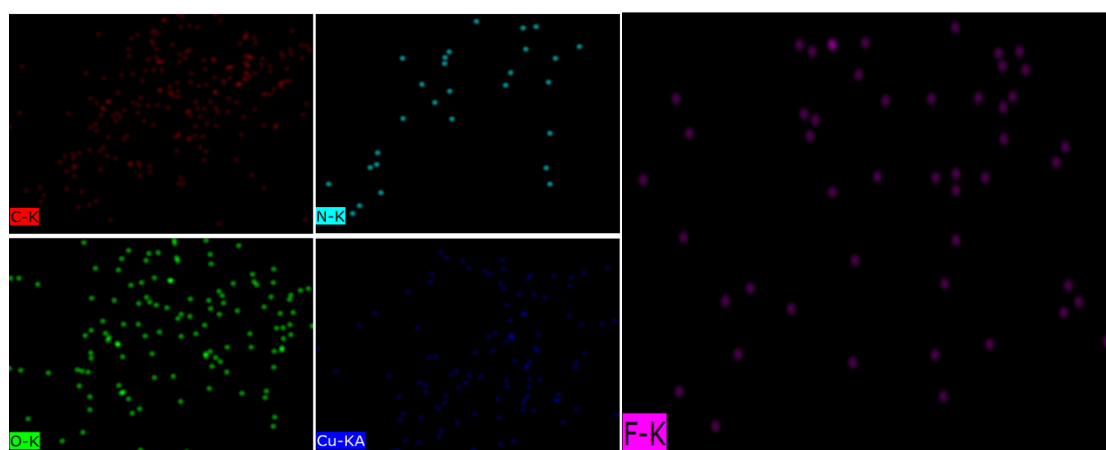


Fig. S2 EDX of the as-synthesized Cu-MOF-F₄.

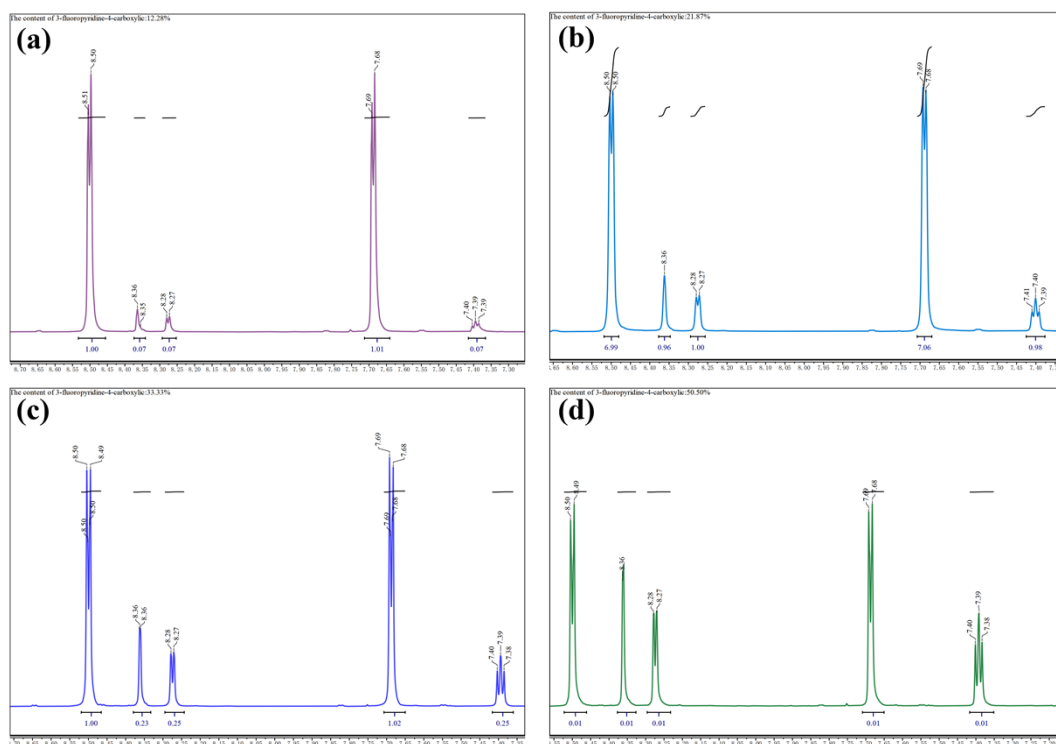


Fig. S3 ^1H NMR spectra of digested (a) Cu-MOF-F₁, (b) Cu-MOF-F₂, (c) Cu-MOF-F₃, and (d) Cu-MOF-F₅ in $[\text{D}_6]$ DMSO.

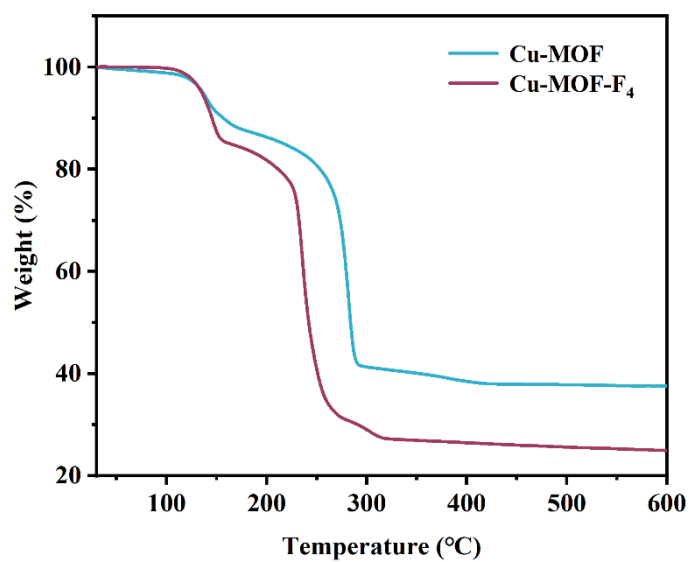


Fig. S4 The TGA of the as-synthesized Cu-MOF and Cu-MOF-F₄.

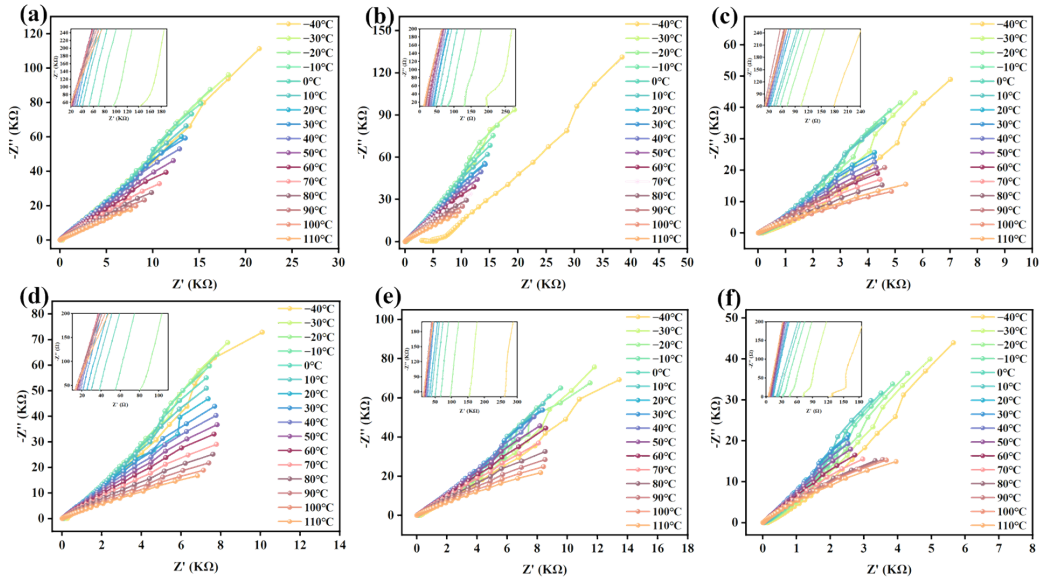


Fig. S5 EIS of (a) Cu-MOF, (b) Cu-MOF-F₁, (c) Cu-MOF-F₂, (d) Cu-MOF-F₃, (e) Cu-MOF-F₄, and (f) Cu-MOF-F₅ electrolyte at temperatures from -40 to 110 °C (the internal is the magnified high frequency area).

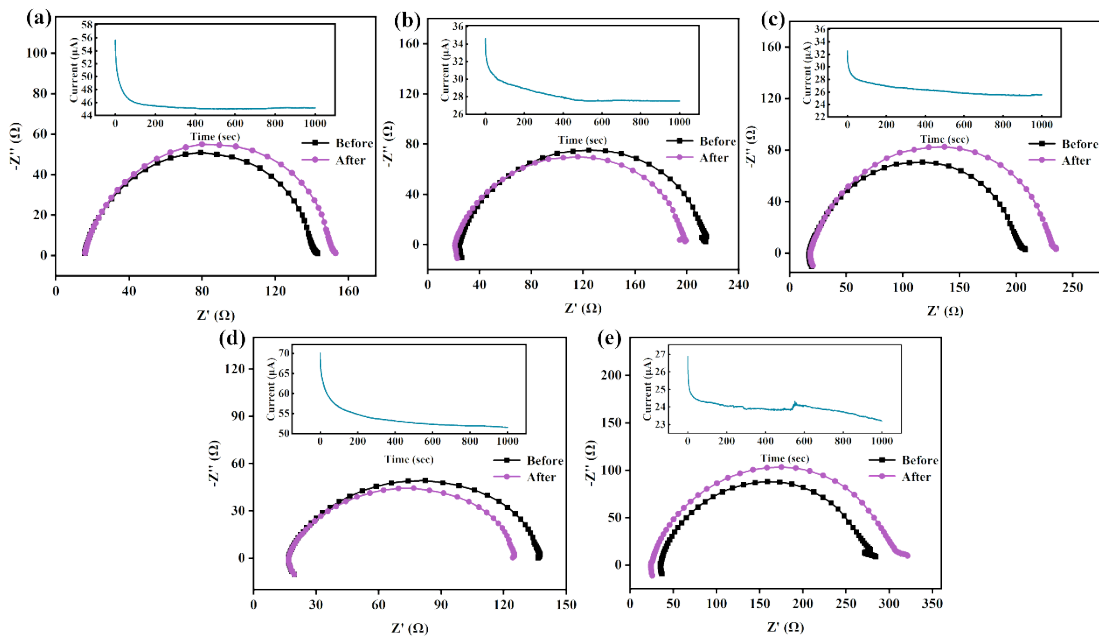


Fig. S6 Chronoamperometric curves and EIS curves of (a) Cu-MOF, (b) Cu-MOF-F₁, (c) Cu-MOF-F₂, (d) Cu-MOF-F₃, and (e) Cu-MOF-F₅ electrolyte before and after polarization.

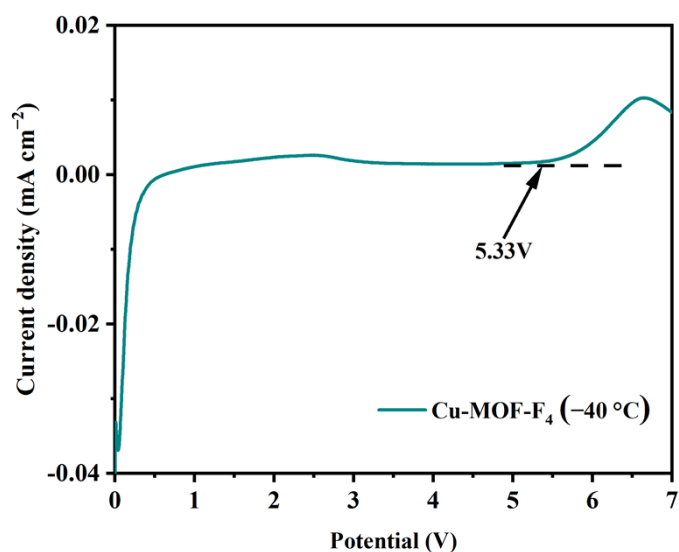


Fig. S7 LSV profiles of Cu-MOF-F_x SSEs sandwiched between Li foil and SS electrodes at -40°C .

Table S1 Tabulated synthetic conditions.

Sample	Ligands		FINA Vs Ligands (%)
	INA (mmol)	FINA (mmol)	
Cu-MOF-F ₁	0.0738	0.00820	10 %
Cu-MOF-F ₂	0.0656	0.0164	20 %
Cu-MOF-F ₃	0.0574	0.0246	30 %
Cu-MOF-F ₄	0.0492	0.0328	40 %
Cu-MOF-F ₅	0.0410	0.0410	50 %

Table S2 Electrolyte uptake of various samples.

Sample	Cu-MOF-F ₄ -1	Cu-MOF-F ₄ -2
M ₁ /g	0.0472	0.0605
M ₂ /g	0.0597	0.0765
(LiPF ₆ + solvent) /g	0.0125	0.0160
(LiPF ₆ + solvent) (wt %)	20.94 %	20.92 %
solvent (wt %)	4.65 %	4.63 %

Table S3 Electrochemical performance of as-prepared Cu-MOF and Cu-MOF-F_x at different temperature.

Temperature	$\cdot\sigma$ (S cm ⁻¹)					
	Cu-MOF	Cu-MOF-F ₁	Cu-MOF-F ₂	Cu-MOF-F ₃	Cu-MOF-F ₄	Cu-MOF-F ₅
-40 °C	2.48×10 ⁻⁶	5.59×10 ⁻⁵	7.40×10 ⁻⁵	5.88×10 ⁻⁵	1.50×10 ⁻⁴	6.24×10 ⁻⁵
-30 °C	6.61×10 ⁻⁵	1.01×10 ⁻⁴	1.40×10 ⁻⁴	1.10×10 ⁻⁴	1.95×10 ⁻⁴	1.10×10 ⁻⁴
-20 °C	1.06×10 ⁻⁴	1.64×10 ⁻⁴	2.20×10 ⁻⁴	1.97×10 ⁻⁴	3.13×10 ⁻⁴	1.82×10 ⁻⁴
-10 °C	1.67×10 ⁻⁴	2.37×10 ⁻⁴	2.84×10 ⁻⁴	3.05×10 ⁻⁴	4.42×10 ⁻⁴	2.74×10 ⁻⁴
0 °C	2.28×10 ⁻⁴	3.27×10 ⁻⁴	3.79×10 ⁻⁴	4.43×10 ⁻⁴	6.04×10 ⁻⁴	3.77×10 ⁻⁴
10 °C	3.10×10 ⁻⁴	4.37×10 ⁻⁴	4.41×10 ⁻⁴	5.94×10 ⁻⁴	7.19×10 ⁻⁴	5.03×10 ⁻⁴
20 °C	3.67×10 ⁻⁴	5.06×10 ⁻⁴	5.77×10 ⁻⁴	6.88×10 ⁻⁴	1.11×10 ⁻³	5.89×10 ⁻⁴
30 °C	3.86×10 ⁻⁴	5.76×10 ⁻⁴	6.92×10 ⁻⁴	8.23×10 ⁻⁴	1.26×10 ⁻³	7.15×10 ⁻⁴
40 °C	4.62×10 ⁻⁴	6.82×10 ⁻⁴	8.05×10 ⁻⁴	9.80×10 ⁻⁴	1.46×10 ⁻³	8.45×10 ⁻⁴
50 °C	5.53×10 ⁻⁴	8.16×10 ⁻⁴	9.40×10 ⁻⁴	1.13×10 ⁻³	1.70×10 ⁻³	1.02×10 ⁻³
60 °C	6.67×10 ⁻⁴	9.75×10 ⁻⁴	1.08×10 ⁻³	1.30×10 ⁻³	1.97×10 ⁻³	1.19×10 ⁻³
70 °C	7.74×10 ⁻⁴	1.12×10 ⁻³	1.23×10 ⁻³	1.49×10 ⁻³	2.19×10 ⁻³	1.39×10 ⁻³
80 °C	8.91×10 ⁻⁴	1.28×10 ⁻³	1.39×10 ⁻³	1.67×10 ⁻³	2.42×10 ⁻³	1.62×10 ⁻³
90 °C	1.01×10 ⁻³	1.44×10 ⁻³	1.54×10 ⁻³	1.85×10 ⁻³	2.63×10 ⁻³	1.78×10 ⁻³
100 °C	1.15×10 ⁻³	1.61×10 ⁻³	1.66×10 ⁻³	2.02×10 ⁻³	2.83×10 ⁻³	1.97×10 ⁻³
110 °C	1.31×10 ⁻³	1.77×10 ⁻³	1.76×10 ⁻³	2.14×10 ⁻³	2.99×10 ⁻³	2.15×10 ⁻³

Table S4 Summary of conductivity of lithium ions electrolytes at low temperatures.

NO.	Materials	σ (S cm ⁻¹)	Temperature	Reference
1	Li-IL@MOF	2.20×10^{-5}	-20 °C	2
2	BStSi	3.10×10^{-5}	-20 °C	3
3	LCMOF-1	3.45×10^{-5}	-20 °C	4
4	Hollow ZIF-8	2.46×10^{-4}	-20 °C	5
5	ZIF-67@ZIF-8	3.44×10^{-4}	-20 °C	6
6	1 M LiFSI BTFE/DME	8.70×10^{-4}	-40 °C	7
7	0.2PESF-0.8LLZTO	1.49×10^{-4}	-10 °C	8
8	CPE-10 % LLZTO	1.30×10^{-4}	0 °C	9
9	L-ILCE	9.00×10^{-5}	-40 °C	10
10	TXEFDMA-LiDFOB	2.20×10^{-4}	-20 °C	11
11	F-PCEE	2.30×10^{-4}	-10 °C	12
12	ACCE	1.30×10^{-3}	-50 °C	13
13	CuBDC-10	7.30×10^{-5}	-40 °C	
14	Cu-MOF-F₄	1.50×10^{-4}	-40 °C	This work
		3.13×10^{-4}	-20 °C	

References

- 1 R. A. Natour, Z. K. Ali, A. Assoud and M. Hmadeh, *Inorg. Chem.*, 2019, **58**, 10912-10919.
- 2 Z. Wang, R. Tan, H. Wang, L. Yang, J. Hu, H. Chen and F. Pan, *Adv. Mater.*, 2018, **30**, 1704436.
- 3 Z. Lin and J. Liu, *RSC Adv.*, 2019, **9**, 34601-34606.
- 4 Q. Zhang, D. Li, J. Wang, S. Guo, W. Zhang, D. Chen, Q. Li, X. Rui, L. Gan and S. Huang, *Nanoscale*, 2020, **12**, 6976-6982.
- 5 L. Tian, Z. Liu, F. Tao, M. Liu and Z. Liu, *Dalton Trans.*, 2021, **50**, 13877-13882.
- 6 Z. Liu, P. Liu, L. Tian, J. Xiao, R. Cui and Z. Liu, *Chem. Commun.*, 2020, **56**, 14629-14632.
- 7 J. Holoubek, K. Kim, Y. Yin, Z. Wu, H. Liu, M. Li, A. Chen, H. Gao, G. Cai, T. A. Pascal, P. Liu and Z. Chen, *Energy Environ. Sci.*, 2022, **15**, 1647-1658.
- 8 J. Sun, M. Tian, H. Dong, Z. Lu, L. Peng, Y. Rong, R. Yang, J. Shu and C. Jin, *Appl. Mater. Today*, 2022, **27**, 101447.
- 9 J. Li, Y. Cai, Y. Cui, H. Wu, H. Da, Y. Yang, H. Zhang and S. Zhang, *Nano Energy*, 2022, **95**, 107027.
- 10 Y. Zhang, J. Huang, H. Liu, W. Kou, Y. Dai, W. Dang, W. Wu, J. Wang, Y. Fu and Z. Jiang, *Adv. Energy Mater.*, 2023, **13**, 2300156.
- 11 Z. Li, R. Yu, S. Weng, Q. Zhang, X. Wang and X. Guo, *Nat. Commun.*, 2023, **14**, 482.
- 12 J. Park, H. Seong, C. Yuk, D. Lee, Y. Byun, E. Lee, W. Lee and B. J. Kim, *Adv. Mater.*, 2024, **36**, 2403191.
- 13 N. Chen, M. Feng, C. Li, Y. Shang, Y. Ma, J. Zhang, Y. Li, G. Chen, F. Wu and R. Chen, *Adv. Funct. Mater.*, 2024, **34**, 2400337.
- 14 X. Wang, S. Jin, L. Shi, N. Zhang, J. Guo, D. Zhang and Z. Liu, *ACS Appl. Mater. Interfaces*, 2024, **16**, 33954-33962.